Optics and Lasers in Engineering 78 (2016) 35–47

Contents lists available at ScienceDirect

Optics and Lasers in Engineering

journal homepage: www.elsevier.com/locate/optlaseng

Programmable Colored Illumination Microscopy (PCIM): A practical and flexible optical staining approach for microscopic contrast enhancement

Chao Zuo [a,b,*], Jiasong Sun [a,b], Shijie Feng [a,b], Yan Hu [a,b], Qian Chen [b]

[a] Smart Computational Imaging Laboratory (SCILab), Nanjing University of Science and Technology, Nanjing, Jiangsu Province 210094, China
[b] Jiangsu Key Laboratory of Spectral Imaging & Intelligent Sense, Nanjing University of Science and Technology, Nanjing, Jiangsu Province 210094, China

ARTICLE INFO

Article history:
Received 28 June 2015
Received in revised form
23 September 2015
Accepted 24 September 2015

Keywords:
Microscopy
Contrast enhancement
Programmable illumination
Optical staining

ABSTRACT

Programmable colored illumination microscopy (PCIM) has been proposed as a flexible optical staining technique for microscopic contrast enhancement. In this method, we replace the condenser diaphragm of a conventional microscope with a programmable thin film transistor-liquid crystal display (TFT-LCD). By displaying different patterns on the LCD, numerous established imaging modalities can be realized, such as bright field, dark field, phase contrast, oblique illumination, and Rheinberg illuminations, which conventionally rely on intricate alterations in the respective microscope setups. Furthermore, the ease of modulating both the color and the intensity distribution at the aperture of the condenser opens the possibility to combine multiple microscopic techniques, or even realize completely new methods for optical color contrast staining, such as iridescent dark-field and iridescent phase-contrast imaging. The versatility and effectiveness of PCIM is demonstrated by imaging of several transparent colorless specimens, such as unstained lung cancer cells, diatom, textile fibers, and a cryosection of mouse kidney. Finally, the potentialities of PCIM for RGB-splitting imaging with stained samples are also explored by imaging stained red blood cells and a histological section.

1. Introduction

In the microscopic examination of transparent colorless specimens such as typical unstained biological samples, it is frequently necessary to employ specific chemical staining or fluorescent labelling before they can be distinctly seen and studied in the microscope [1]. However, these exogenous contrast agents are not always desirable because they may perturb the natural state and function of the live specimens. Together with the costs of labeling agents and complexity in specimen preparation, this is a fundamental motivation for favoring non-phototoxic label/stain-free imaging techniques.

Optical contrast-enhancing imaging techniques, such as dark field, Zernike phase contrast, oblique illumination, as well as Rheinberg illumination are established as widely used standard label-free techniques for visualization of such colorless transparent specimens at the optical resolution limit [2]. Despite the differences of their imaging properties, all of these methods require spatially-modulated illuminations by introducing additional physical masks and optical filters before the condenser lens of the microscope. For example, in dark-field microscopy, a spider stop is inserted into the aperture focal plane of the condenser to create a hollow cone of illumination with larger numerical aperture compared to that of the objective lens. In Zernike phase-contrast microscopy, an annulus, also known as a phase ring, is introduced in the aperture plane of the condenser to make the conjugate area fit the ring-shape phase plate inside the phase-contrast objective lens. The Rheinberg illumination, known as optical staining, modifies dark-field and bright-field sections in the dark-field stop with colored filters to provide rich contrasting colors to both the specimen and background [3]. Though all of those methods enable a direct visualization of cells and other colorless transparent specimens without staining, several limitations are prevalent: a change in imaging modality is generally accompanied by filter replacement and optical re-alignment, precluding dynamic multi-modal imaging for live samples. On the other hand, a great number of physical masks and optical filters are required to match objective lenses with a range of magnifications for different types of illuminations, necessitating a bulky condenser turret. Besides, to accumulate such filter sets especially for Rheinberg filters with different color combinations can be prohibitively expensive.

* Corresponding author.
E-mail addresses: surpasszuo@163.com (C. Zuo), chenq@njust.edu.cn (Q. Chen).

http://dx.doi.org/10.1016/j.optlaseng.2015.09.009
0143-8166/

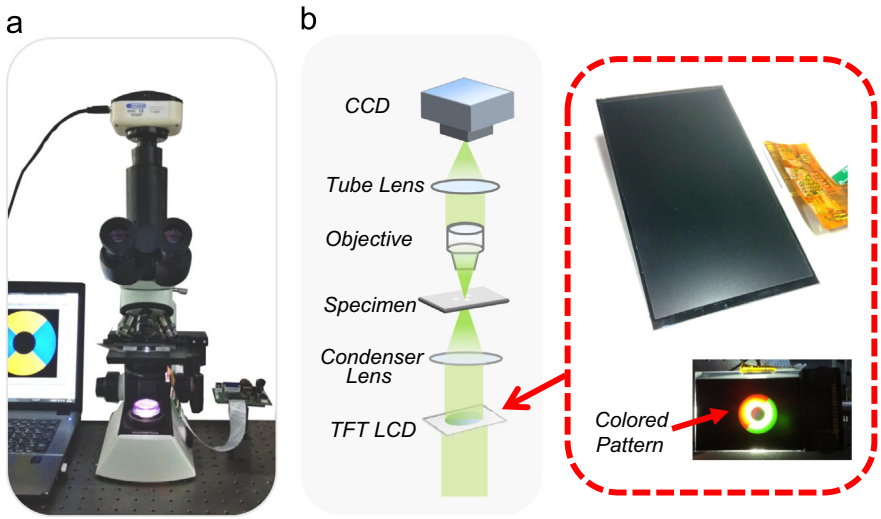

Fig. 1. The PCIM system. (a) Photograph of the whole system. (b) Schematic illustration of the optical configuration.

Recent advances in LED lighting and digital display technology provide new opportunities for active digital illumination control for advancing microscopy. By integrating a high-resolution spatial light modulator (SLM) or a video projector into the illumination path of the microscope, one gains the flexibility to produce sophisticated illumination patterns or dynamically switchable illumination sources with no physically moving parts [4–7]. However, since the SLM is a technically complex device, these systems end up being heavy, bulky, and expensive. Alternatively, the active illumination control can be realized by replacing the condenser with a ring or matrix of LEDs [8–10]. The LED-based condenser-free scheme provides a simple and cost-effective solution to realizing multi-modal contrast enhancement imaging but with a significantly reduced light collecting efficiency. Recently, the use of a low cost liquid crystal display (LCD) to achieve programmable condenser illumination control has been reported [11]. This technique has the advantages of being cost-effective, light efficient, and easy to incorporate into most standard bright-field microscopes. However, the twisted nematic LCD used in their prototype setup can only provide binary light amplitude modulation, which makes it impossible for more complicated color phase-contrast imaging, such as Rheinberg illumination.

In this paper, we present the Programmable Colored Illumination Microscopy (PCIM) to achieve multi-modal and flexible optical staining for microscopic contrast enhancement. The PCIM is an improvement to the previously reported LCD based scheme that uses an amorphous Silicon (a-Si) thin film transistor (TFT) LCD to realize high-resolution spatial modulation of both *amplitude* and *color* of the light at the condenser aperture plane of the microscope. The ease of generating different colored illumination filters with the TFT-LCD opens the possibility to realize more well-established imaging modalities and the possibility to develop new optical color contrast staining methods. The implemented methods are performed to increase image contrast of complementary structures in several transparent colorless specimens, such as unstained lung cancer cells, textile fibers, and a slice of mouse kidney. In additional, the feasibility of utilizing PCIM in RGB-splitting and multi-shot photomicrography for color stained specimen is also demonstrated, taking advantage of the spectral selectivity within the TFT-LCD.

The contents of this paper are organized as follows: Section 2 describes the system setup for PCIM. Several important optical characteristics of the PCIM system, including optical alignment, illumination spectrum, color reproductivity, contrast ratio, and imaging resolution are characterized and presented in Section 3.

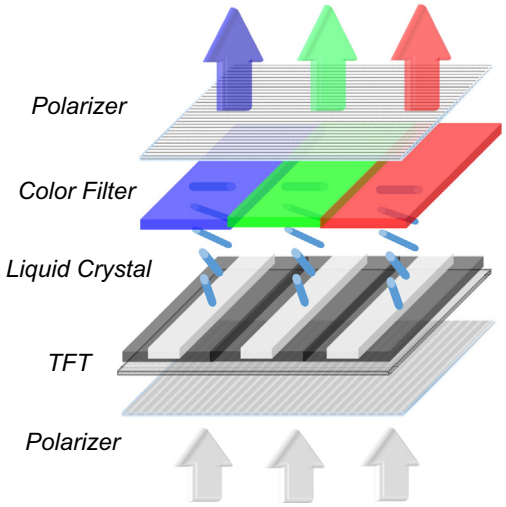

Fig. 2. Schematic illustration of single pixel cell structure of the TFT-LCD.

Practical applications of the PCIM system for contrast-enhancement imaging, optical staining, and RGB-splitting imaging are illustrated in Section 4. Section 5 gives the conclusions.

2. System setup for PCIM

The PCIM system is built based on a commercial infinity-corrected microscope (Olympus CX22). Fig. 1(a) shows a photograph of the PCIM system. The schematic layout of the optical configuration is shown in Fig. 1(b). The light from the built-in halogen lamp passes a color temperature conversion filter to produce daylight-balanced illuminations. The commercial infinity-corrected microscope is composed of a condenser associated with aperture diaphragm, objective, and tube lens. The images are acquired using a cooled CCD camera (Qimaging, Micro Publisher 5.0, 2560×1920, 3.4 μm pixels, 12 bit). The key component of PCIM, a commercially available a-Si TFT-LCD module, contains two primary components: a color TFT panel and a backlight unit. We remove the backlight unit of the LCD and leave only the color TFT-LCD panel as a low-cost transmissive spatial light modulator, arranged at the aperture plane of the condenser lens (replace the original physical aperture diaphragm). The panel size is 4.3 inch and the pixel resolution is 480×272. Fig. 2 shows a schematic cell

structure of the TFT-LCD. The liquid crystal (LC) layer is sandwiched between a-Si TFT substrate and a color filter substrate. Two orthogonally aligned polarizers are attached to the outer faces of the panel. An individual TFT drives the LC molecules to alter the polarization properties of a pixel to control the light transmittance when displaying information content. Since the LC molecule itself does not produce color, an array of color filters with spectral transmittances corresponding to three primary colors, red, green, and blue (RGB), needs to be placed after the LC layer. This divides each pixel of the display into three cells or sub-pixels which are colored RGB. Each sub pixel can be controlled to yield 16.7 millions (24-bit) of possible colors for each pixel. The whole TFT-LCD module is controlled by computer software via USB with an STM32 microcontroller.

3. Optical characterization of PCIM system

3.1. Optical alignment

To guarantee a successful implementation of PCIM, the TFT-LCD should be well aligned so that the displayed patterns can be projected precisely into the objective's back focal plane. By use of a Bertrand lens or phase telescope, the proper centering of the displayed pattern can be visually controlled. Fig. 3 illustrates the experimental setup for imaging the objective rear aperture. Compared with Fig. 1(b), an additional lens is used for obtaining the image of the objective's back focal plane. In the following test, we choose to use a phase-contrast objective (Olympus, LUCPLFLN 20X, $NA_{obj}=0.45$) for the system alignment since the inner phase ring is quite helpful for precisely locating the center of the objective's back focal plane.

To establish the correspondence between LCD pixels and objective's back focal plane pixels, we can adopt the approach that is widely used for the calibration of structured light system for 3-D shape measurement [12]. In this approach, sinusoidal phase-shifted fringe patterns with different fringe pitch are generated in a computer and displayed on the TFT-LCD. Based on a multi-frequency phase-shifting algorithm [13], the absolute phase at each pixel can be calculated, which can be used to find a line of corresponding pixels on the LCD. If both vertical and horizontal fringe patterns are used, then the pixel at the intersection of these two lines is the corresponding pixel of the LCD. Fig. 4 shows several back focal plane images when the vertical and horizontal sinusoidal fringes with different frequencies are displayed on the TFT-LCD. Based on this approach, correspondence between LCD pixels and objective's back focal plane pixels can be established. Alternatively, we can also align the LCD pattern by simply displaying a white circle that is just larger than the phase contrast ring, and then observe the corresponding back focal plane image. Then the pattern can be shifted to precisely into the center of the objective's back focal plane with the help of the phase contrast ring, as demonstrated in Fig. 5. In this way, the center of the pattern can also be aligned with optical axis conveniently. It should be noted that for those pixels situated outside the objective NA, they are not visible in the image but still useful to produce dark-field contrast.

3.2. Illumination spectrum and color reproductivity

As we have shown in Section 2, different colors of the LCD is reproduced by proper combination of the three additive primary colors, red, green, and blue. When a “white” image is displayed on the TFT-LCD employed, the spectrum content of the illumination cover the 400–700 nm range, as shown in Fig. 6, measured by a

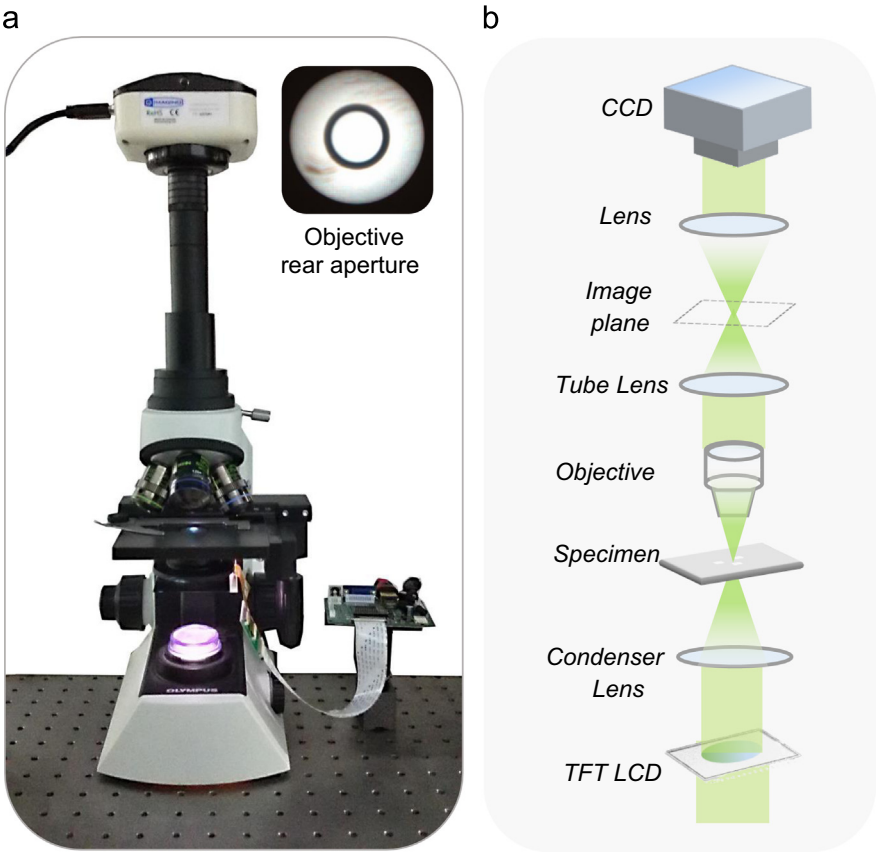

Fig. 3. Experimental configuration for imaging the objective rear aperture. (a) Photograph of the experimental system. (b) Schematic illustration of the optical configuration.

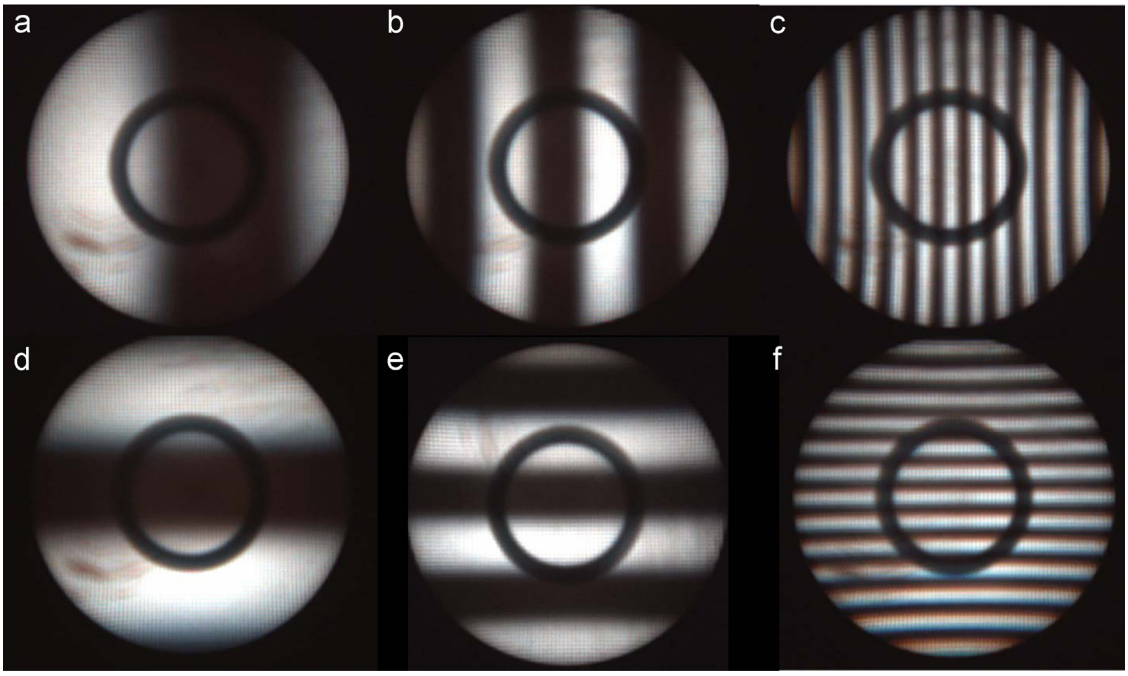

Fig. 4. Captured back focal plane images when the vertical (a–c) and horizontal (d and e) sinusoidal fringes with different frequencies are displayed on the TFT-LCD.

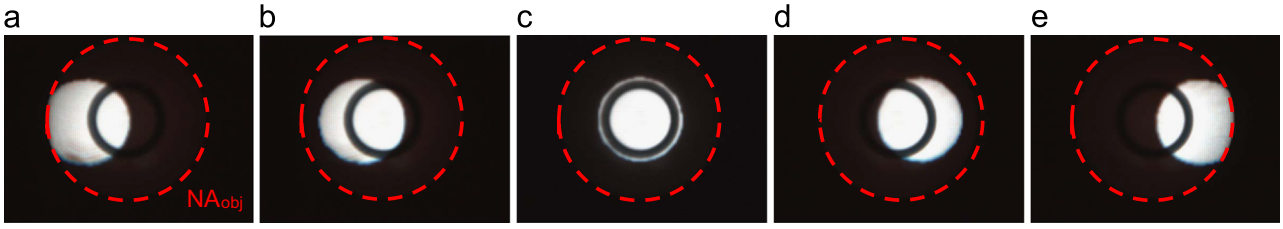

Fig. 5. Back focal plane images when the pattern displayed on the LCD is horizontally displaced (a,b,d,e), and optimally aligned with optical axis (c). The red dashed circle NA_{obj} delineates the region within the numerical aperture of the objective lens. (For interpretation of the references to color in this figure caption, the reader is referred to the web version of this paper.)

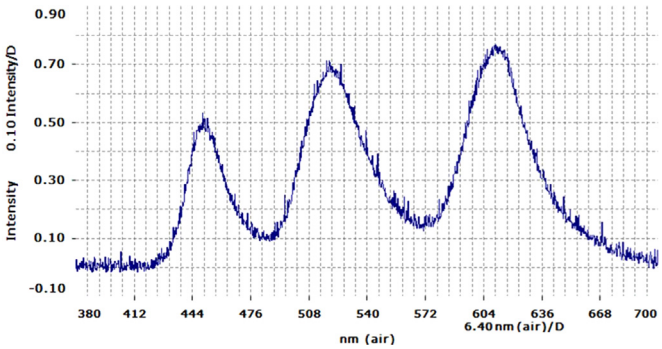

Fig. 6. The spectral response of the illumination when a "white" image is displayed on the TFT-LCD.

spectrometer (Thorlabs CCS200). Evidently, there are three spectral bands where there are only very few spectral overlaps between adjacent colors: for red, green, and blue channels, respectively. The average peak wavelengthes are at 617 nm, 525 nm, and 456 nm, which match the peak transmissions of typical color filters quite precisely. The minimal overlap and the absence of strong spectral tails may help create narrow-band quasi-monochromatic illuminations for RGB-splitting imaging, as will be demonstrated in Section 4.3. Furthermore, Fig. 7 shows the back focal plane image when a test color disk image is displayed on the LCD, which demonstrates a very good color reproduction of the LCD screen. Accurate color reproduction is extremely important for achieving high image quality and color consistency in color-contrast optical staining microscopy. But it should be noted that the color referred in this work is not 'true' color (as in hyperspectral imaging); it is only a combination of three different spectral channels corresponding to the visual primary colors red, green and blue. Hence, the final color image obtained is not quantitative, which must be carefully distinguished from the conventional quantitative fluorescence microscopy techniques.

3.3. Contrast ratio

Since the TFT-LCD employed in our PCIM system acts as a transmissive spatial light modulator, ideally the light transmittance of each pixel on the 'off-state' should be zero (no light can pass through). However, the truth is there is always a small amount of light leakage via non-lit pixels, which leads to a residue background of the captured image. The light leakage effect can be quantified by the 'contrast ratio', which is defined as the "white" transmittance divided by the "black" transmittance of the LCD screen. The contrast ratio of the TFT-LCD employed in our PCIM is measured to be 412:1 with use of a simple "full on/full off" method, which is slightly lower than the advertised specifications (600:1). The transmittance in 'on-state' is measured to be about 17% (the ratio between the light intensity with and without the TFT-LCD). The losses of light may result from the absorptive

polarizers, absorption of light reflected from thin-film transistors (TFTs), and absorption of light by pigments used in the color filters.

3.4. Image resolution

It is well accepted that the commercial microscope from major companies can deliver diffraction-limited image quality. As we demonstrated in Section 2, the PCIM system replaces the 'physical' condenser aperture diaphragm with a 'digital' TFT-LCD screen to achieve both amplitude and color modulation across the condenser aperture plane of the microscope. It is hoped that the additional flexibility is gained without compromising the diffraction-limited imaging resolution of the original microscope. To study the microscopic resolution of the PCIM system, we apply a standard U.S. Air Force (USAF) resolution test target as the test sample. The test target is illuminated by using the original condenser (with 'physical' condenser aperture diaphragm) and the modified digital condenser (with the TFT-LCD screen), respectively. For a fair comparison, the test target is imaged using the same objective 10× plan semi-apochromat objective (Olympus, UPLANFLN 10X, $NA_{obj}=0.3$) with matched illumination (both the 'physical' and the 'digital' condenser aperture diaphragm are set to the same size as the objective aperture). Fig. 8 shows the experimental results, with the insets showing magnified views of the raw data. The pixel size of the image is 0.34 μm at the object plane (CCD pixel size divided by the magnification factor). The finest feature of group 9, element 3 on the USAF target (0.78 μm line width) is clearly resolved in both cases. The intensity cross-sections along the marked lines obtained for the PCIM system and unmodified microscope are compared in Fig. 8(c). Only a slight dip (about 15%) in intensity modulation can be observed when the two cross-sections are carefully compared. Those results allow us to say at most, our PCIM prototype can achieve a similar diffraction-limited microscopic resolution to a conventional

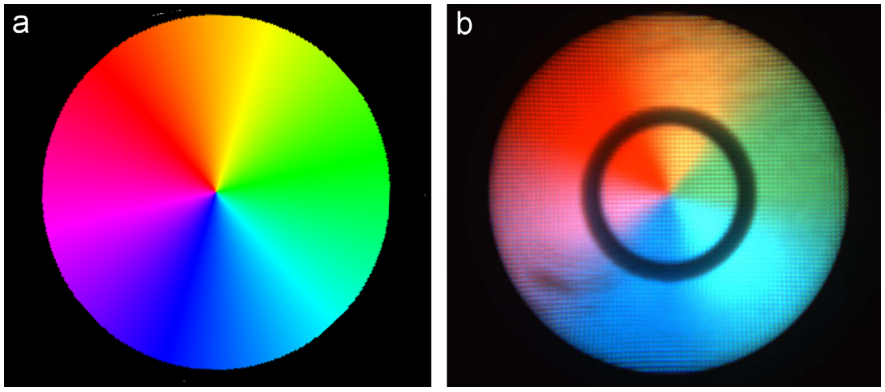

Fig. 7. The back focal plane image when a test color disk image is displayed on the TFT-LCD. (For interpretation of the references to color in this figure caption, the reader is referred to the web version of this paper.)

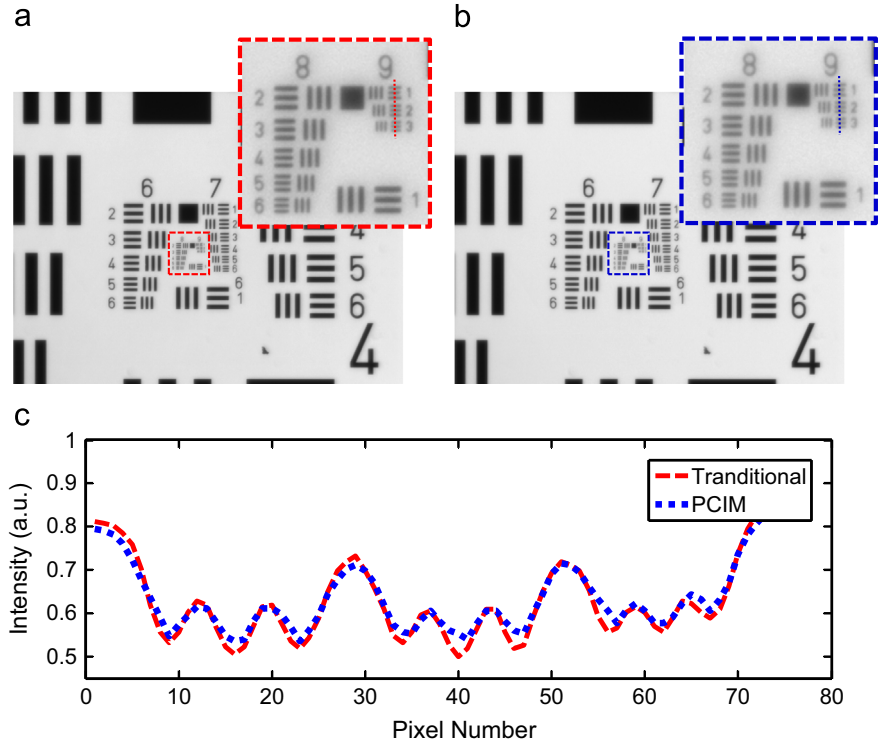

Fig. 8. Image resolution test with a USAF target (Olympus, UPLANFLN 10X, $NA_{obj}=0.3$). (a) Conventional non-modified microscope. (b) PCIM system. (c) Intensity cross-sections along the marked lines. The insets show corresponding magnified views of the raw data.

microscope, following the Rayleigh resolution limit ($\lambda/2\mathrm{NA} \approx 0.76\ \mu\mathrm{m}$).

4. Results in practical applications of PCIM

4.1. Contrast-enhancement imaging with binary and gray-scale patterns

We first demonstrate the flexibility of the PCIM to realize several classical microscope techniques such as bright field, dark field, Zernike phase contrast, and oblique illumination by displaying only binary and gray-scale patterns on the LCD. The test sample is unstained lung cancer cell (LC-06), which is imaged by an long working distance semi-apochromat phase-contrast objective with magnification 20× (Olympus, LUCPLFLN 20XPH, $\mathrm{NA}_{obj}=0.45$).

Bright-field imaging can be implemented straightforwardly by just displaying a clear circle on the LCD. The diameter of this circle determines the spatial coherence of the illumination (illumination aperture). Fig. 9 shows bright-field images of unstained cells with different illumination apertures NA_{ill}. Using a small radius improves the image contrast at the expense of lateral resolving power. Increasing the circle size improves the spatial resolution as well as the depth-sectioning ability, which is equivalent to opening up the condenser aperture diaphragm in a traditional microscope. In Fig. 10, we show the corresponding objective back focal plane images by displaying white circles with different sizes on the LCD. In the PCIM system, such an adjustment process can be performed digitally without any mechanical switching. Furthermore, the ability to modulate the 2D amplitude across the aperture plane of the condenser allows to use Gaussian functions as the illumination aperture apodization for bright-field imaging, as we demonstrated in Fig. 9(d). It can be observed that the cells are difficult to visualize under bright field (even though the illumination aperture is small) because they absorb/refract too little light to produce sufficient contrast.

For dark-field imaging, a complementary central black circle is displayed that physically block out the zero-order illuminating beam from directly entering the objective. The diameter of the central stop should be just greater than the numerical aperture of the objective, which can be controlled by observing the objective back focal plane (Fig. 12(b)). This dark-field imaging process is similar to adding a dark-field aperture stop at the condenser diaphragm. The increase in contrast is evident in Fig. 11(b), where the details inside the cells are clearly highlighted in white against a dark background. The structures having high spatial frequencies are emphasized and only light scattered by the sample contributes

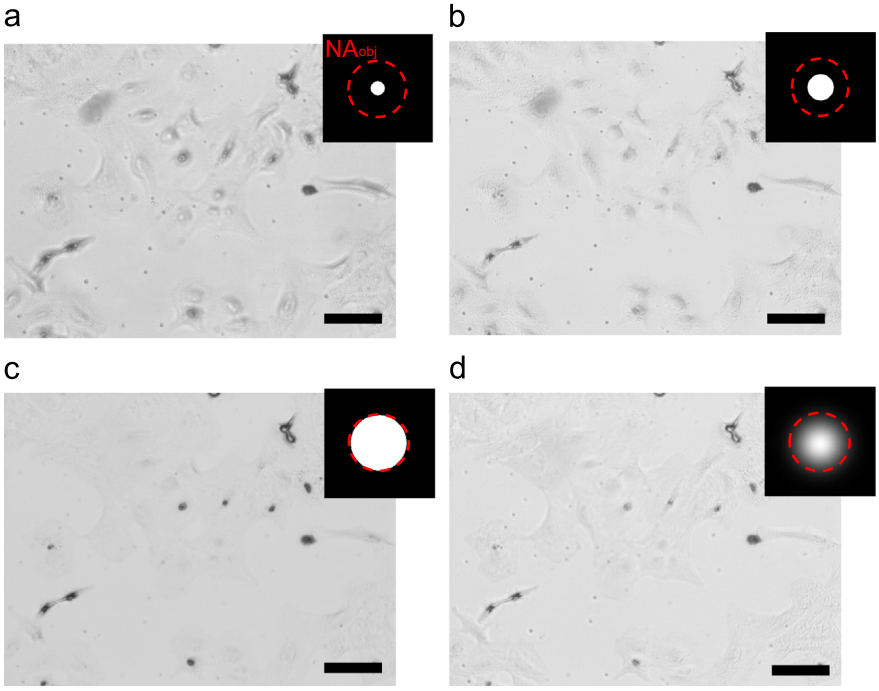

Fig. 9. Bright-field imaging of unstained lung cancer cells (LC-06) with different illumination apertures. (a) $\mathrm{NA}_{ill}=0.2\mathrm{NA}_{obj}$. (b) $\mathrm{NA}_{ill}=0.5\mathrm{NA}_{obj}$. (c) $\mathrm{NA}_{ill}=1.0\mathrm{NA}_{obj}$. (d) Gaussian apodization. The insets show the corresponding patterns displayed on the LCD. The red dashed circle NA_{obj} shows the numerical aperture of the objective lens. Scale bar 50 μm. (For interpretation of the references to color in this figure caption, the reader is referred to the web version of this paper.)

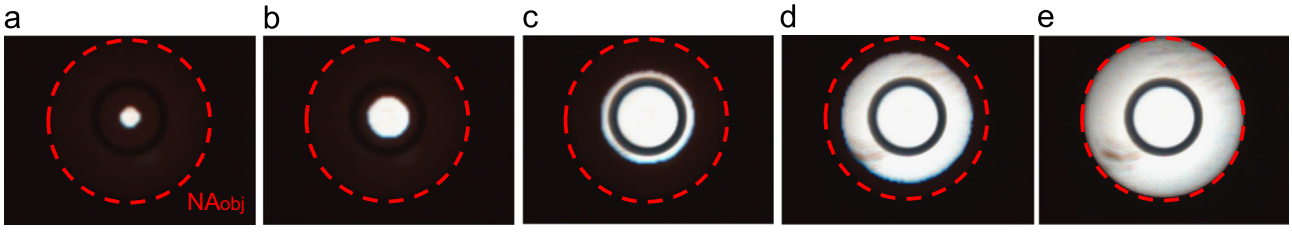

Fig. 10. Varying the illumination aperture by displaying white circles with different sizes on the TFT-LCD. (a) $\mathrm{NA}_{ill}=0.15\mathrm{NA}_{obj}$. (b) $\mathrm{NA}_{ill}=0.3\mathrm{NA}_{obj}$. (c) $\mathrm{NA}_{ill}=0.55\mathrm{NA}_{obj}$. (d) $\mathrm{NA}_{ill}=0.8\mathrm{NA}_{obj}$. (e) $\mathrm{NA}_{ill}=1.0\mathrm{NA}_{obj}$.

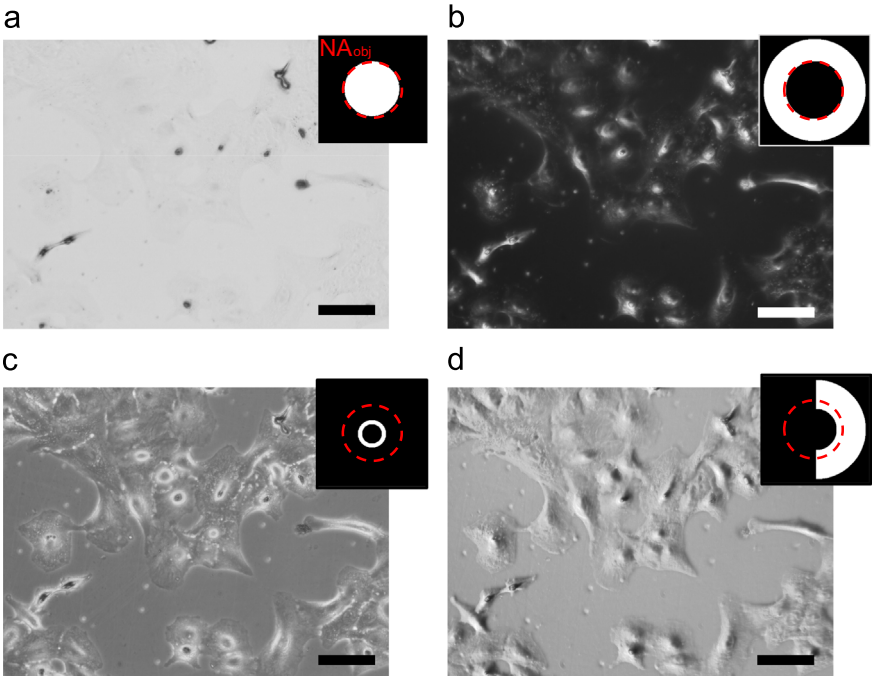

Fig. 11. Contrast-enhancement imaging of unstained lung cancer cell (LC-06). (a) Bright field ($NA_{ill}=NA_{obj}$). (b) Dark field. (c) Phase contrast. (d) Oblique illumination. The insets show the corresponding patterns displayed on the LCD. The red dashed circle NA_{obj} shows the numerical aperture of the objective lens. Scale bar 50 μm. (For interpretation of the references to color in this figure caption, the reader is referred to the web version of this paper.)

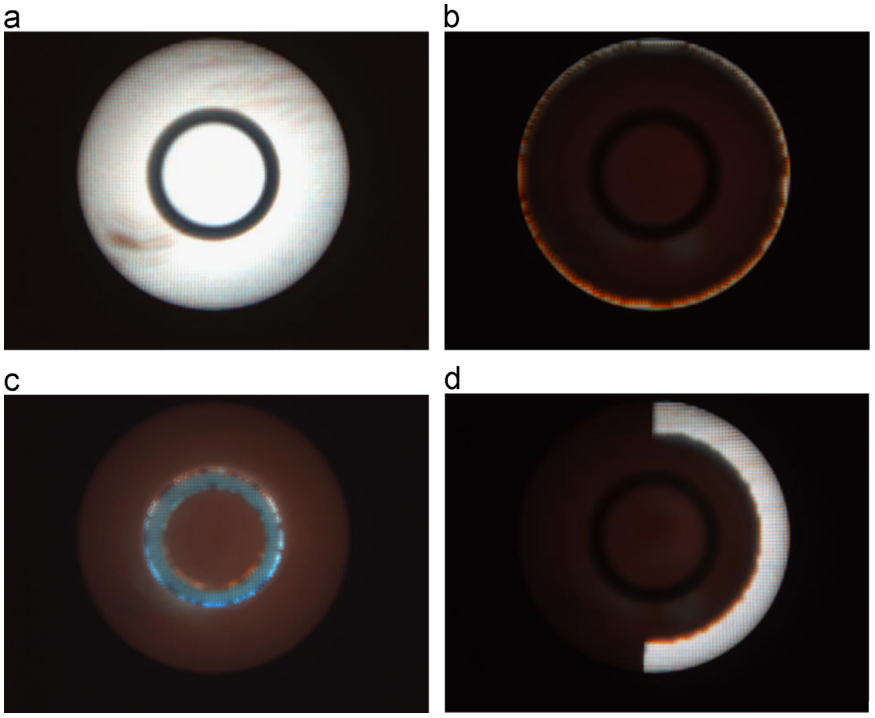

Fig. 12. Objective back focal plane images for different imaging modalities. (a) Bright field ($NA_{ill}=NA_{obj}$). (b) Dark field. (c) Phase contrast. (d) Oblique illumination. (For interpretation of the references to color in this figure caption, the reader is referred to the web version of this paper.)

to image formation. In standard dark-field microscopy, the central ray is physically blocked by an opaque stop which rejects the unscattered illumination completely and results in a ideal dark field of view or background. However, with the PCIM setup, the degree of the background darkness depends on the contrast ratio of the TFT-LCD, which is 412:1 as we measured in Section 3.3. This contrast ratio is enough to produce a sufficiently dark background. Furthermore, the residual background can also be digitally removed from the measurements by background subtraction (with a additional sample-free image).

The principle of the Zernike phase-contrast method is to shift the phase of the unscattered light in a way that it interferes with the scattered light to convert the phase information into amplitude information. In conventional phase contrast microscopy, the illumination is isolated using an annulus in the aperture plane of the condenser. A phase ring built into the objective at the back

focal alters the phase of the undiffracted illuminating light without affecting the diffracted light. With the PCIM setup, by displaying a ring-type pattern that matches the annular phase plate in the back focal plane of the phase contrast objective, a phase contrast image can be obtained without using any physical annuli (Fig. 12(c)). Its appearance reveals the differences of refractive index and thickness of microscopic structures, with typical bright 'halo' surrounding the cell periphery (Fig. 11(c)). It should be noted that the size of the phase contrast annuli depends on the magnification of the objective lens and separate annulus masks must be paired with different objectives. With the PCIM setup, the amplitude pattern can easily be re-sized and even nudged under computer control to accommodate magnification changes and alignment requirements, eliminating the need for any additional optics and physical masks required in traditional illuminators.

The phase-contrast microscopy commonly used in visualization of phase objects does not deliver the quasi-3D effect and introduces a disturbing halo effect around the edges. Another contrast enhancement approach, so-called oblique illumination, however, uses asymmetric illumination aperture to create the high-contrast pseudo-relief imaging effects (Fig. 11(d)), thus facilitating their comprehension by the human visual system. As shown in Fig. 12 (d), an off-axis white pattern was utilized to setup oblique illumination. For phase objects like cells, the intensity profiles in the oblique illumination roughly correspond to the optical path difference gradients in the apparent direction of illumination. With the flexibility of the PCIM setup, the white sector in the illumination pattern can also be easily rotated to any azimuthal angle to highlight different directional structures in the sample.

4.2. Optical staining with color patterns

Not just limited to binary patterns, the TFT-LCD is also able to adjust color and intensity level of the light passing through each single pixel, which opens more flexibilities in optical color contrast imaging. As a classic form of optical staining, Rheinberg illumination is able to render the normally colorless specimen with rich color against a contrasting background by replacing the central opaque stop of the dark field microscope with a transparent color filter [2,3]. The peripheral ring around the central disk is also a filter of contrasting color (e.g., a blue annulus surrounding a yellow circle). Rheinberg illumination can be viewed as a multiplexed bright-field and dark-field imaging since the central cone and the surrounding hollow cone of light simultaneously produce an image. Thus the central filter becomes the background color while the fine structure of the specimen is highlighted by the color of the outer ring. Fig. 13 shows the procedure of adjusting the displayed pattern for Rheinberg illumination (blue-yellow); the diameter of the inner blue circle is gradually increased until it is just greater than the aperture of the objective. This process is similar to adjusting the annular size for dark-field imaging. As shown in Fig. 14(a), Rheinberg illumination of unstained cells using a blue central filter and a yellow annular ring causes an increased contrast effect, similar to dark field, but with a pleasant colored background. Zeroth-order light from the blue central filter pervades the background. The edges and fine details of cells scatter the yellow component, which accentuate these higher-spatial-frequency structures. Similarly, if we use a green annulus around a red central filter, the cells would appear green in a red background, as illustrated in Fig. 14(b).

Rheinberg illumination is also well suited for examination of small diatom frustules. The capability of the PCIM for high quality imaging of low density diatom at high magnification is presented in Fig. 15. In this experiment, a very small diatom shell is observed with a 60× magnification phase contrast objective (Olympus, UPlanFLN 60X, 1.25NA, Oil, Iris). This diatom has a center-to-center frustule spacing (spacing between the dotted lines) of approximately 0.4–0.5 μm. Note the oil immersion objective used here has an internal iris diaphragm at its rear focal plane, so that the NA_{obj} can be easily adjusted within the range of 0.65–1.25. Such an iris is also helpful for realizing Rheinberg illumination microscopy in high magnification and oil-immersion optics. In this configuration, the illumination patterns were displayed on the LCD with the maximum possible size (maximum illumination NA is 0.9/dry,

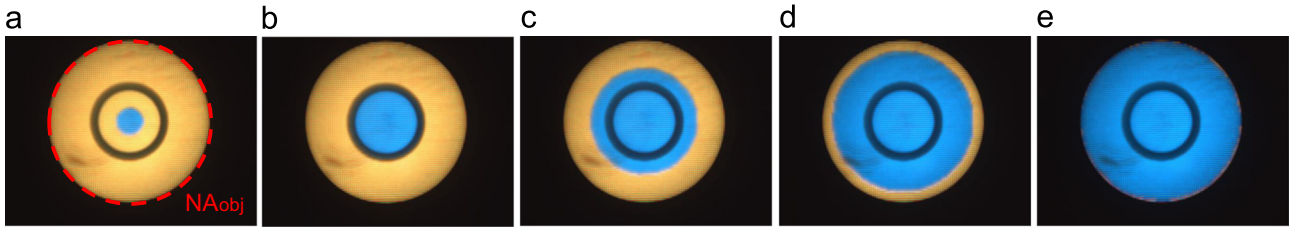

Fig. 13. Adjusting the displayed pattern for Rheinberg illumination. The diameter of the inner circle is increased until it just greater than the aperture of the objective. (For interpretation of the references to color in this figure caption, the reader is referred to the web version of this paper.)

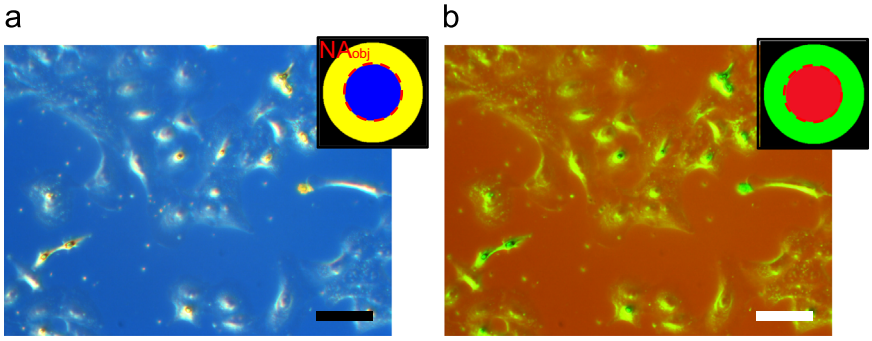

Fig. 14. Imaging of unstained lung cancer cell (LC-06) with Rheinberg illumination. (a) Rheinberg illumination (blue-yellow). (b) Rheinberg illumination (red-green). The red dashed circle NA_{obj} shows the numerical aperture of the objective lens. Scale bar 50 μm. (For interpretation of the references to color in this figure caption, the reader is referred to the web version of this paper.)

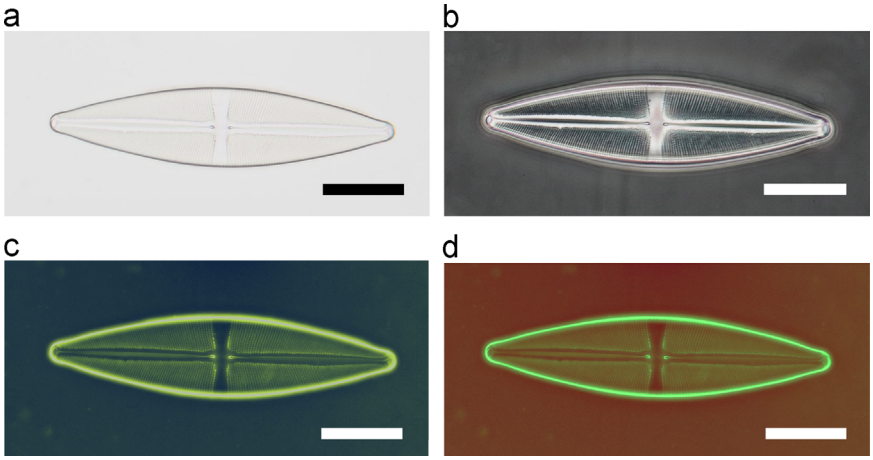

Fig. 15. Contrast-enhancement imaging of a diatom. (a) Bright field. (b) Phase contrast. (c) Rheinberg illumination (blue-yellow). (d) Rheinberg illumination (red-green). Scale bar 20 μm. (For interpretation of the references to color in this figure caption, the reader is referred to the web version of this paper.)

Fig. 16. Contrast-enhancement imaging of textile fibers. (a) Bright field (blue). (b) Bright field dominated Rheinberg illumination. (c) Equalized Rheinberg illumination. (d) Dark field dominated Rheinberg illumination. (e) Dark field (yellow). Scale bar 100 μm. (For interpretation of the references to color in this figure caption, the reader is referred to the web version of this paper.)

determined by the condenser lens used). Then the iris diaphragm is adjusted until the outer ring of light falls out of the viewfield at the rear focal plane of the objective. As is shown in Fig. 15(a), the diatom frustule appears in low contrast in bright field because of its low density. In phase contrast, the fine internal pattern is much better contrasted, but the individual pores on the frustule cannot be well resolved because of haloing (Fig. 15(b)). While in Rheinberg illuminations (Fig. 15(c) and (d)), not only the marginal contours of the diatom is visualized in a distinct manner, but the small pores on the frustule appear sharply demarcated.

It is important to note that in designing Rheinberg filters, the transmittance of the central circle should be much darker than the outer ring in order to enhance the overall contrast and the visibility of detailed structure. Otherwise, the effects of the dark field component on the resultant image will be swamped out by the background signal. In our system, the optimal contrast of the image can be fine-tuned by gradually attenuating the brightness of the central filter and retaining its color unchanged to achieve a smooth transition from bright-field to dark-field illumination. Figs. 16 gives an overview of the variance in contrast and background achievable when compared with colored bright field (blue) (Fig. 16(a)) and dark field illumination (yellow) (Fig. 16(e)). Furthermore, it is also possible to divide the outer ring of the Rheinberg filter into alternating sectors of colors. As shown in Fig. 17(c), the outer part of the disk is divided into two halves (red and green), and the central filter then is filled with blue. Such tricolored Rheinberg illumination are particularly effective in examining objects that show pronounced periodic structure. Fig. 17(d) shows another variant of Rheinberg filter where the annulus is divided into four quadrants of alternating colors (yellow and blue). In this example, the Rheinberg illumination techniques yield remarkably better contrast and clarity than does bright field.

Besides Rheinberg illumination, the flexibility of the LCD also allows for superposition of different aperture patterns, virtually allowing to crossbreed any microscopic techniques, whose combination in a traditional physical setup would be laborious if possible at all [14,15]. The combined method is expected to inherit the advantages of both techniques while their typical shortcomings can be alleviated. Fig. 18 presents several examples of those combined filters by imaging a unstained slice of mouse kidney. Dark-field imaging can be combined with small-aperture bright-field imaging to achieve high spatial resolution and large depth-of-focus simultaneously (Fig. 18(b)). Moreover, low- to moderate-density specimens can appear in a phase-contrast like manner but free from haloing. The phase-contrast imaging can be combined with dark-field imaging to gain additional resolving power and more fine details (Fig. 18(c)). Bright-field imaging can be combined with oblique illumination to deliver high contrast pseudo-relief image against a colored background (Fig. 18(d)). The respective illuminating light components associated with bright field, dark field, phase contrast, and oblique illumination can be filtered at different colors, and their intensity can be selectively regulated so that the final image can be dominated by one illumination mode or be equalized.

The freely programmable TFT-LCD also offers the possibility to develop new filters for contrast enhancement. We present here two heuristically developed filters. The iridescent dark-field imaging is related to conventional dark-field imaging, as the specimen is illuminated with high-angle hollow light cone, but the transparent dark-field annular ring is replaced by a color wheel (Fig 18 (e)). The color circle based on spectral wavelengths appears with red at one end of the spectrum and violet at the other. Conventional dark-field imaging is known to be an isotropic imaging method, but in iridescent dark-field imaging, complementary colors are located directly opposite each other on the color wheel, converting dark-field imaging to an anisotropic color contrast enhancement method. Unlike the ordinary dark-field imaging, the asymmetric color illumination contributes to image formation,

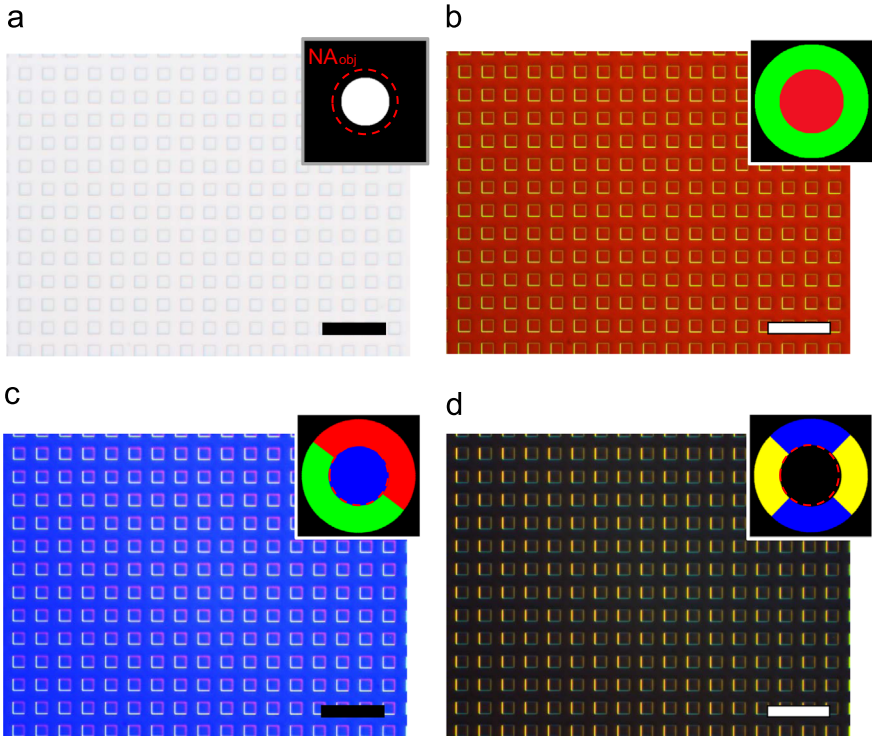

Fig. 17. Contrast-enhancement imaging of a transparent object with periodic structure. (a) Bright field. (b-d) Rheinberg illuminations of different types. The insets show the corresponding patterns displayed on the LCD. Scale bar 50 μm. (For interpretation of the references to color in this figure caption, the reader is referred to the web version of this paper.)

leading to shadowing and apparent three-dimensional structures. The colorful quasi-3D image of the mouse kidney cryosection gives the impression that the specimen has a certain (apparent) thickness, especially the distal tubules in the cortex, and tissue ruffling. Structures with different azimuthal angles are optically stained with different and contrasting colors: for example, the Bowman's capsules may appear red on a single side while green on the opposing side. The direction of the color contrast depends on the orientation of the color wheel, which can be precisely adjusted under electronic control (see Video 1) to highlight different structures in the sample or study the effect of rotation on image formation. The iridescent phase-contrast imaging, similarly, convert the conventional phase-contrast imaging into an anisotropic color contrast enhancement method by substituting condenser annulus with a color wheel of the same size (Fig 18(f)). The iridescent phase-contrast imaging produces a brilliantly colored and aesthetically beautiful image. However, it still suffers from extensive halo artifacts that overwhelmingly blur the structural details, especially edges. Comparatively, the iridescent dark field is better suited for examining considerably thicker specimens than it is reasonably possible under the phase contrast which performs well only on relatively thin specimens (a few μm).

4.3. *RGB-splitting imaging for stained samples*

In the previous sections, the capability of the PCIM system has been demonstrated with unstained colorless specimens. In this subsection, we explore the potentialities of using the PCIM system for color imaging with stained samples. As we shown in Section 2, all pixels in the TFT-LCD are coated with color filters for red, green, or blue. These filters can be used to create quasi-monochromatic illumination for light microscopy. This can be regarded as interesting tools for photomicrography of stained samples that can maximize the quality of true color imaging based on RGB-splitting and multi-shot techniques [16]. Fig 19 presents red blood cell samples stained with hematoxylin and eosin (H.& E.), photographed with a minimally corrected achromatic objective (Olympus, PLN40X, 0.65NA), taken in normal halogen light without using any color balance filter, monochromatic red, green, and blue illuminations. It is evident that the monochromatic images lead to visible improvement of sharpness and contrast, especially for the green and blue illuminations (Fig. 19(c) and (d)). Since the red blood cells are stained red, they are barely visible under red illumination (Fig. 19(b)). These three monochrome images taken in red, green, and blue can be further superimposed, so that a color image can be reconstructed, as shown in Fig. 20(e). In this case, any degradation of the image quality caused by potential chromatic aberration associated with all components of the optical system (microscope objectives, tube lens and the digital camera) can be minimized. Furthermore, since the R,G,B images are captured separately, the balance and purity of color can be optimized in a superior manner, and deviations in color tinge are minimized. The color adjustment achievable by RGB-splitting imaging can be made more accurate and precise than those resulting from manipulations of the color or white balance based on camera presets or the usual image processing software.

Further improvements of the image sharpness can be achieved when each monochrome single image is focused separately and individually. In color photomicrography, the focal plane may significantly differ with regard to the dominant color or wavelength. This phenomenon is referred as “chromatic defocus” and previously has been used for quantitative phase imaging [17,18] and depth sectioning in a microscope [19,20]. This focal plane shift can be up to a few microns when the color is changed from red or green to blue. Thus, in a single exposure, images on a single focal plane can be regarded as a compromise. However, in RGB-splitting imaging, the optimum focal plane for different colors can be adjusted separately, and thus all

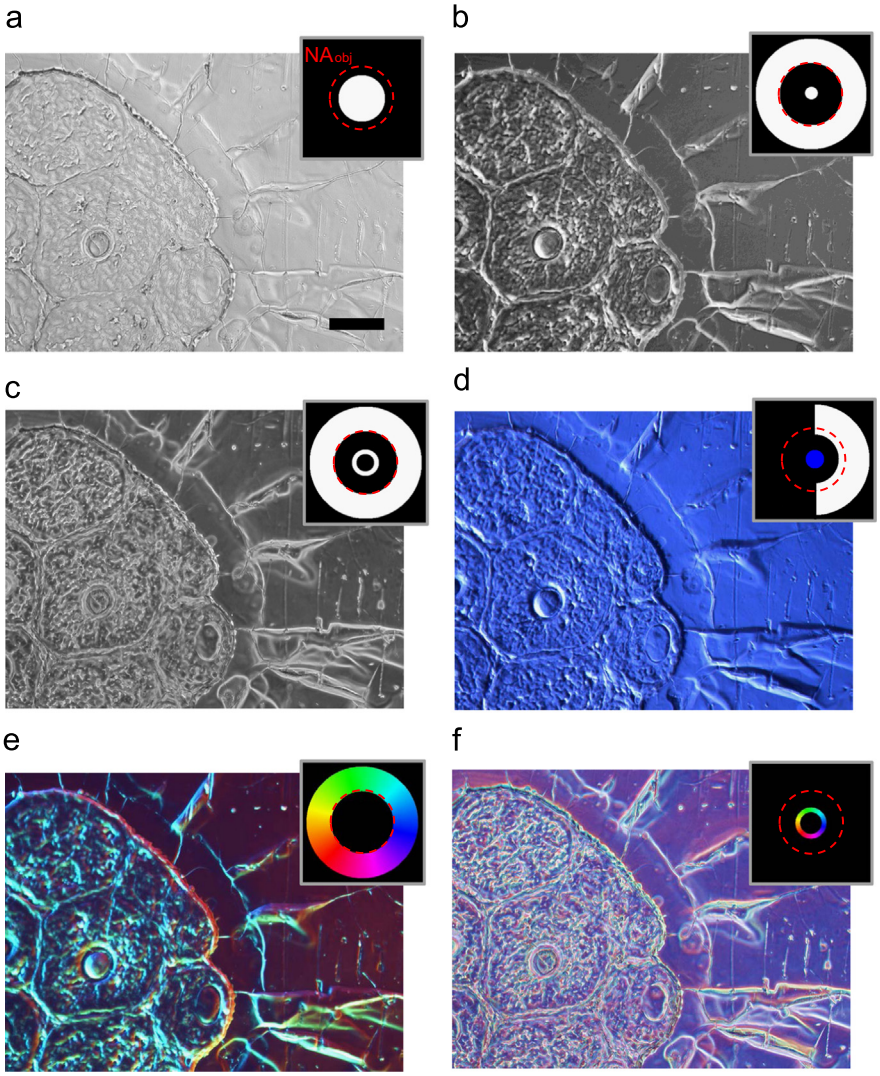

Fig. 18. Contrast-enhancement imaging of a unstained slice of mouse kidney. (a) Bright field. (b) Bright field + dark field. (c) Phase contrast + dark field. (d) Bright field + oblique illumination. (e) Iridescent dark field (Video 1). (f) Iridescent phase contrast. The insets show the corresponding patterns displayed on the LCD. Scale bar 100 μm. (For interpretation of the references to color in this figure caption, the reader is referred to the web version of this paper.)

structures can be ideally focused. Fig. 20 presents another example (a stained tissue section of squamous cell carcinomas) of RGB-splitting imaging, in which improvement of image sharpness can be perceived. Besides, any relevant deviations related with the hue of color (yellowish tint of halogen light) can be well corrected in ideal tones.

5. Conclusions

In conclusion, we have demonstrated a flexible microscopic setup, PCIM, to realize numerous color contrast imaging methods by utilizing a TFT-LCD as a low-cost colored transmissive spatial light modulator located at the condenser aperture plane of the microscope. The well-established imaging modalities, such bright field, dark field, phase contrast, oblique illumination, and Rheinberg illumination can be easily achieved by simply creating different colored patterns displayed on the LCD. Switching between different imaging modalities can be performed purely electronically without re-alignment and any moving parts. Furthermore, the PCIM opens the possibility of combining multiple microscope techniques to improve the image quality and information content, or even realizing completely new methods for optical color contrast staining, such as iridescent dark-field imaging and iridescent phase-contrast imaging. The versatility and effectiveness of PCIM has been demonstrated by imaging of several transparent colorless specimens, such as unstained lung cancer cells, diatom, textile fibers, and a cryosection of mouse kidney.

The RGB color filter of the TFT-LCD was then utilized to achieve RGB-splitting and multi-shot photomicrography. It leads to visible improvements in sharpness, resolution and color balance, and any loss of quality caused by potential chromatic aberration can be avoided. In multi-color specimens, all structures will be ideally focused, as the optimum focal plane will no longer be dependent on the regional color or dominant wavelength. The color balance and purity can be optimized in a superior manner, and deviations in color tinge are minimized. Those positive effects have been demonstrated by imaging stained red blood cells and a histological section.

At the moment we only scratched at the surface of the possibilities. A wealth of new illumination filters and imaging capabilities will arise if one really exploits the power of programmable illumination in a more thorough way. We also only used the LCD in the illumination path of the microscope. However, it is also possible to use LCD panel as a spatial light modulation in the imaging path of the microscope. In this way, even more imaging

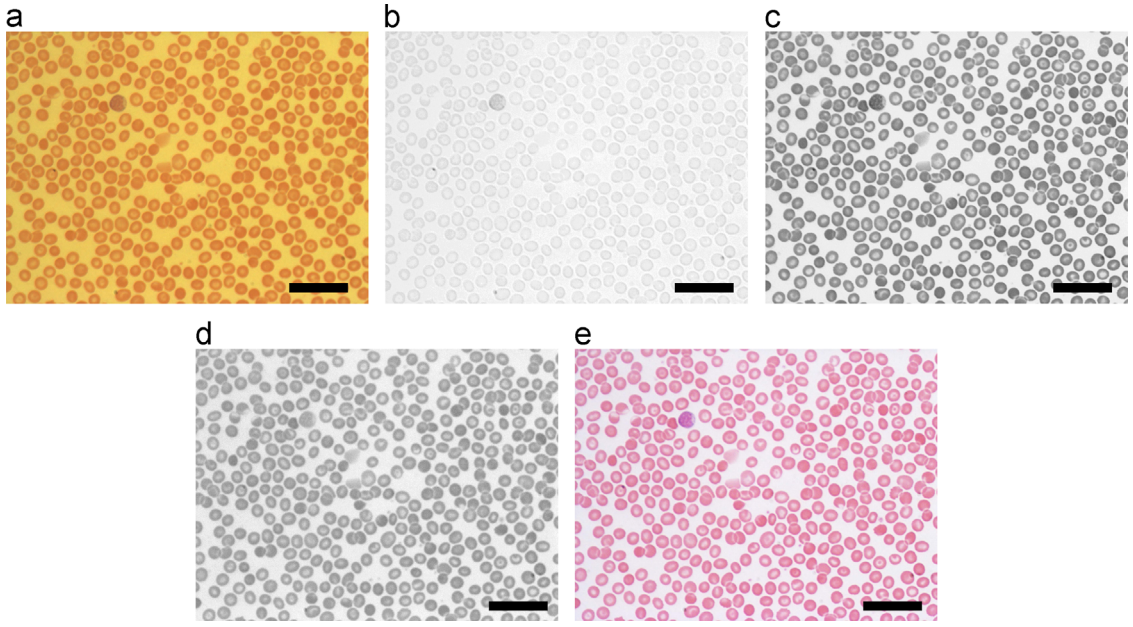

Fig. 19. H. & E. Stained red blood cell sample. (a) Single shot image taken without color temperature conversion filter. (b–d) Monochrome images taken with narrow band R, G, B illuminations, respectively. (d) RGB reconstruction from (b–d). Scale bar 30 μm. (For interpretation of the references to color in this figure caption, the reader is referred to the web version of this paper.)

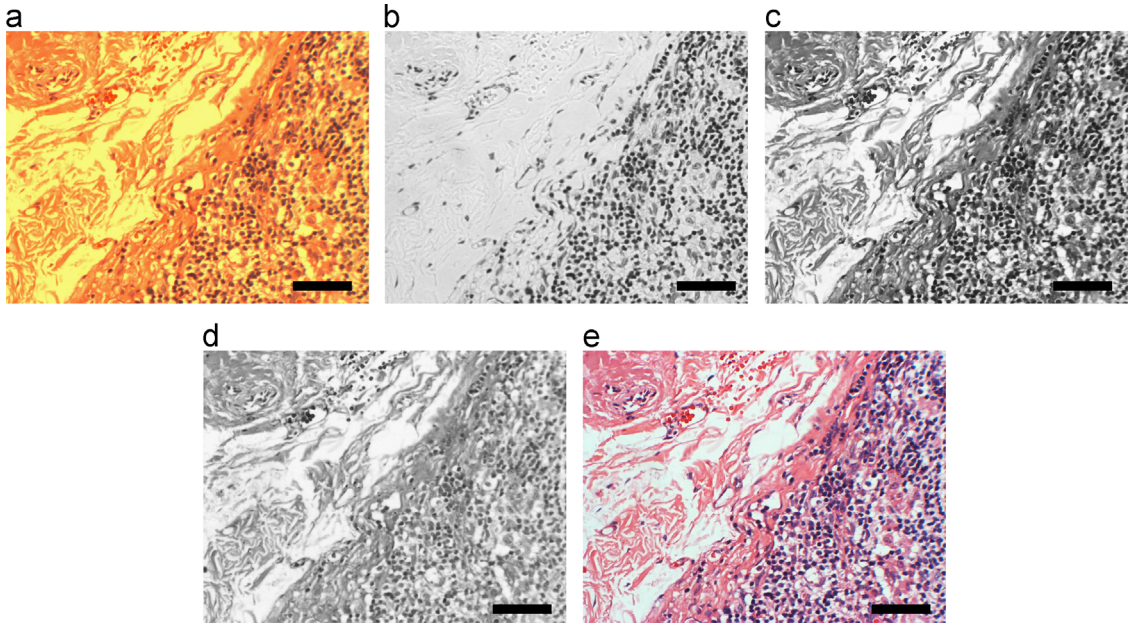

Fig. 20. H. & E. stained tissue section of squamous cell carcinoma. (a) Single shot image taken without color temperature conversion filter. (b–d) Monochrome images taken with narrow band R, G, B illuminations, respectively. (d) RGB reconstruction from (b–d). Scale bar 30 μm. (For interpretation of the references to color in this figure caption, the reader is referred to the web version of this paper.)

methods can be achieved in a flexible way by programming the LCD.

Finally, it should be mentioned that one limitation of the PCIM system lies in the low transmittance in 'on-state' of the LCD screen. This transmittance is measured to be about 17% in our prototype setup, and thus, the light transmission efficiency is only 17% of the conventional microscope that uses a traditional condenser illuminator. Consequently, most of light produced by the halogen light source is absorbed and converted into heat across the LCD panel. The light waste problem is even more severe when the pixels in the LCD are not fully on. For example, in the phase-contrast imaging, most light is blocked by the non-lit pixels and only a very small portion of light within the annulus region contributes to image formation (this problem also exists in standard phase contrast microscopy that using a physical condenser annulus). But the relative light efficiency our approach is still much higher than the LED-based condenser-free schemes [8–10] (for a typically arrangement, only less than 1% of light can enter the objective to produce a image). With the rapid development in the display technology, the transmittance and the contrast ratio of the LCD will still improve. In that case, we fully expect the LCD-based programmable illumination techniques will transform the light microscope into a more flexible, efficient, and multi-functional research tool.

Acknowledgements

This work was supported by the National Natural Science Fund of China (11574152, 61505081, and 11574152), “Six Talent Peaks” project (2015-DZXX-009, Jiangsu Province, China) and '333 Engineering' research project (BRA2015294, Jiangsu Province, China), Fundamental Research Funds for the Central Universities (30915011318), and Open Research Fund of Jiangsu Key Laboratory of Spectral Imaging & Intelligent Sense (3092014012200417). C. Zuo thanks the support of the 'Zijin Star' program of Nanjing University of Science and Technology..

Appendix A. Supplementary data

Supplementary data associated with this paper can be found in the online version at http://dx.doi.org/10.1016/j.optlaseng.2015.09.009.

References

[1] Mertz J. Introduction to optical microscopy. Roberts and Company Publishers: Boston; 2010.
[2] M. Pluta, Specialized methods, advanced light microscopy. Vol. 2. Elsevier; 1989.
[3] Rheinberg J. On an addition to the methods of microscopical research, by a new way optically producing color-contrast between an object and its background, or between definite parts of the object itself. J R Microsc Soc 1896;16:373–88.
[4] Samson EC, Blanca CM. Dynamic contrast enhancement in widefield microscopy using projector generated illumination patterns. New J Phys 2007;9:363.
[5] Warber M, Zwick S, Hasler M, Haist T, Osten W. SLM-based phase-contrast filtering for single and multiple image acquisition. Proc SPIE 2009;7442: 74420E.
[6] Maurer C, Jesacher A, Bernet S, Ritsch-Marte M. What spatial light modulators can do for optical microscopy. Laser Photon Rev 2011;5:81–101.
[7] Steiger R, Bernet S, Ritsch-Marte M. SLM-based off-axis Fourier filtering in microscopy with white light illumination. Opt Express 2012;20:15377–84.
[8] Zheng G, Kolner C, Yang C. Microscopy refocusing and dark-field imaging by using a simple LED array. Opt Lett 2011;36:3987–9.
[9] Liu Z, Tian L, Liu S, Waller L. Real-time brightfield, darkfield, and phase contrast imaging in a light-emitting diode array microscope. J Biomed Opt 2014;19:106002.
[10] Webb KF. Condenser-free contrast methods for transmitted-light microscopy. J Microsc 2015;257:15377–84.
[11] Guo K, Bian Z, Dong S, Nanda P, Wang Y, Zheng G. Microscopy illumination engineering using a low-cost liquid crystal display. Biomed Opt Express 2015;6:574–9.
[12] Zhang S, Huang PS. Novel method for structured light system calibration. Opt Eng 2006;45:083601–8.
[13] Zuo C, Chen Q, Gu G, Feng S, Feng F, Li R, et al. MHigh-speed three-dimensional shape measurement for dynamic scenes using bi-frequency tripolar pulse-width-modulation fringe projection. Opt Laser Eng 2014;59:56–71.
[14] Piper T, Piper J. Variable Phase-darkfield Contrast (VPDC) C a variant illumination technique for improved visualizations of transparent specimens. Microsc Microanal 2012;18:343–52.
[15] Piper T, Piper J. Universal variable brightfield-darkfield contrast: a variant technique for improved imaging of problematic specimens in light microscopy. Microsc Microanal 2012;19:1092–105.
[16] Piper J. RGB-splitting and multi-shot techniques in digital photomicrography-utilization of astronomic RGB-filters in true color imaging. Microsc Today 2009;17:48–51.
[17] Waller L, Kou SS, Sheppard CJR, Barbastathis G. Phase from chromatic aberrations. Opt Express 2010;18:22817–25.
[18] Zuo C, Sun J, Zhang J, Hu Y, Chen Q. Lensless phase microscopy and diffraction tomography with multi-angle and multi-wavelength illuminations using a LED matrix. Opt Express 2015;23:14314–28.
[19] Molesini G, Quercioli F. Pseudocolor effects of longitudinal chromatic aberration. J Opt (Paris) 1986;17:279–82.
[20] Courtney-Pratt JS, Gregory RL. Microscope with enhanced depth of field and 3-D capability. Appl Opt 1973;12:2509–19.